Chapter 4 - Grid Generation and Grid Resolution Studies

4.1 Summary

Several three-dimensional grids were generated in support of the site-scale flow and transport modeling effort. Both structured and unstructured grids were developed, tested, and used for sensitivity analyses and flow calibration studies. Structured grids, commonly referred to as finite-difference grids, are easy to generate but their blocklike structure makes it difficult to represent complicated geometries with all but the finest grid resolution. Unstructured grids, like the common finite-element meshes, are more complicated and may consist of triangles and tetrahedrals. They can, however, represent complicated hydrostratigraphy and topography accurately at fairly low resolution. The hydrostratigraphy represented in the geologic model consists of multiple layers of contrasting fluid flow and transport properties. The grid-generation methods used in the present study allow the stratigraphy to be honored in numerical grids of different resolution so that comparison studies can be performed to test for grid quality and to determine the resolution required for flow and transport simulations. All mesh generation and manipulation is done with the GEOMESH/X3D toolkit (Gable et al., 1995, 1996; Trease et al., 1996).

A series of six structured grids of increasing resolution were used to compare the flow through the model domain to assess the point at which increasing resolution no longer influences the results. This process identifies the resolution required for an accurate simulation of the flow field. A similar study for two unstructured grids demonstrated that the coarser grid used for calibrating the flow model was sufficiently resolved for accuracy. Finally, this chapter reports on the development of a technique for selectively refining the numerical grid for transport calculations. The method uses the solute transport pathway determined on a coarse grid to identify regions of the model where increased grid resolution is required. The mesh-generation software refines the grid in those areas. After two or more successive applications of this process, the grid is finely resolved along the pathways of

solute plume movement, and numerical error associated with insufficient grid resolution is minimized. This technique is demonstrated in a simplified three-dimensional model, and the process is then described for the site-scale model grid. The main application of this technique will be for refining the revised site-scale model for transport calculations.

4.2 Software and Data QA Status

The FEHM code is used to perform all flow and transport calculations in this report. The code is qualified in accordance with Los Alamos quality-assurance (QA) requirements and is documented in several reports by Zyvoloski et al. (1992, 1996b–d). The QA status of the data used in this chapter is shown in Table 4-1.

Table 4-1. QA Status of Data used in this Chapter

REFERENCE	QA Status	DTN/ Assession Number		COMMENT
Czarnecki, J. B., et al. 1997. Preliminary three-dimensional finite-element groundwater flow model of the saturated zone, Yucca Mountain, Nevada. USGS YMP milestone number SP23NM3.	non-Q			
Clayton, R. W., et. al. 1997. ISM2.0: A 3-D geological framework and integrated site model of Yucca Mountain: Version ISM1.0, Doc ID B00000000-01717-5700-00004, Rev. 0, MOL. 19970122.0053. CRWMS M&O,	Q	MOL. 19970122.0053		By agreement with DOE and NRC, accepted as Q even though it uses some non-Q data.
Zelinski, W. P., and R. W. Clayton. 1996. A 3-D geological framework and integrated site model of Yucca Mountain: Version ISM1.0, Doc ID B00000000-01717-5700-00002, Rev. 1. CRWMS M&O.	non-Q			

4.3 Introduction

This chapter addresses the construction of computational grids that reflect complex geologic structure for saturated-zone flow and transport simulations. The importance of grids can be summarized with the following questions:

- What resolution is required to represent geology?
- What resolution is required to represent flow and transport processes?
- Can a grid be optimized to represent features and flow processes while keeping the size relatively small?
- If a flow model is calibrated on a coarse grid, is it calibrated on a fine grid?

These grids must accurately represent the geologic structure and be appropriate for numerically accurate simulations of flow and transport. That is, any error associated with numerical grid discretization must be constrained within specified truncation error tolerances. Understanding the quality of the grids and the effects of grid-related error is necessary for assessing the quality of the simulations and generating a defensible model.

The process of developing flow and transport models for the saturated-zone studies can be divided into three parts:

- Developing accurate conceptual models of the geology and hydrologic material properties.
- Building the grid and prescribing boundary and initial conditions.
- Applying the computational physics models of flow, heat transport, and chemical transport.

Geologic interpretation, stratigraphic model development, and material characterization are performed based on numerous field measurements. The stratigraphic model populated with hydrologic material properties then provides the basis for computational grid development. The ability of the numerical grid to represent the geologic complexity directly affects accuracy of the numerical model's approximation of the actual physical system's response.

GEOMESH/X3D (Gable et al., 1995, 1996; Trease et al., 1996) is a mesh-generation toolkit that can use the hydrostratigraphic model as input to create a numerical grid that represents accurately complex structures and stratigraphy such as faults, pinchouts, and layer truncations. As well as representing geologic structure, this software maintains and distributes physical and chemical attributes such as porosity, permeability, or percent zeolite. The process of populating the numerical grid with hydrologic and transport properties is described in Robinson et al.,1997.

The process of generating and populating numerical grids from geologic framework models is automated, thus making the entire process easy to implement with fewer user-induced errors. At any step in the process, greater numerical resolution can be added to a particular subregion, new boundary conditions can be prescribed, or new attributes can be incorporated.

The grid-quality control issues involved in this automated process cannot be over-emphasized. We believe that a system that uses only electronic processing of the hydrogeologic data is desirable for a defensible model during the licensing process because the interfaces can be qualified and metrics of goodness of representation can be established. These metrics would likely include a volume comparison between the project database hydrogeologic units and the model hydrogeologic units.

As part of our study, we are interested in analyzing how accurately grids of increasing resolution capture this complex structure and simulate flow. At what resolution is the geometry of the material distribution accurately represented with a structured grid in order to model fluid flow through the aquifer? Because higher grid resolution is more computational expensive, we can use this information to determine what the desired accuracy of the result is and at what resolution of grid that accuracy would be attained.

4.4 Saturated-Zone Unstructured Mesh from Stratamodel Geological Model

Software has been developed to automate the steps required to create a finite-element mesh for flow and transport calculations from a geological framework model.

The steps required to create a grid are:

- Convert Stratamodel Stratigraphic Framework Model (SFM) provided by USGS to hexahedral finite-element grid.
- Remove zero volume elements from data structure.
- Remove elements with vertical height less than one meter.
- Convert hexahedral elements to tetrahedral elements.
- Add the points defining the potentiometric surface (surface provided by the USGS).
- Add nodes with specified *xyz* location for measured well-head calibration.
- Add nodes above and below well-head calibration nodes to enhance grid quality.
- Add buffer zones above potentiometric surface and below bottom boundary.
- Assign material values to all nodes.
- Optimize the grid connectivity to insure positive finite-element coefficients.
- Calculate Voronoi control volumes.
- Output node coordinates, node connectivity, nodal volumes, and material and boundary lists.

All file conversion, gridding, node distribution, property interpolation, quality checking, and output is carried out within a single integrated gridding tool kit. This approach insures that the steps taken are reproducible and traceable and modifications to any step in the gridding process can be done without a great deal of labor.

4.5 Grid Generation and Property Interpolation

Generation of grids and interpolation of properties from the hydrostratigraphic model onto the numerical grids is performed with GEOMESH/X3D. GEOMESH/X3D is also used for comparing results from different grids, each having different resolution or grid structure. Interpolation with GEOMESH/X3D allows for the superposition on mesh A of the attributes (material number, pressure, saturation, concentration, etc.) belonging to mesh B. This utility is useful when refining a mesh or when comparing meshes of different resolution. The meshes should generally be of the same volume but do not have to coincide exactly. They do not have to have the same discretization, resolution, or element type. Either mesh can be structured or unstructured. For interpolation, a node of mesh A is first located within an element of mesh B. The attributes of the nodes defining the element in mesh B are then linearly interpolated to the node in mesh A. Output of mesh A from GEOMESH then contains the new attribute values associated with each node. If desired, the mesh-A node is also assigned the material number of the mesh-B element. Elements of mesh A can then be assigned material numbers based on the nodal material numbers that were interpolated from mesh B.

The saturated-zone model domain selected for this grid resolution study is defined by Nevada State Coordinates of 533,340 m to 563,340 m in an east-west direction, 4,046,782 m to 4,091,782 m in the north-south direction, and –754 to 1332 m vertically above sea level. Nineteen materials are assumed located within this volume as shown in Figure 4-1.

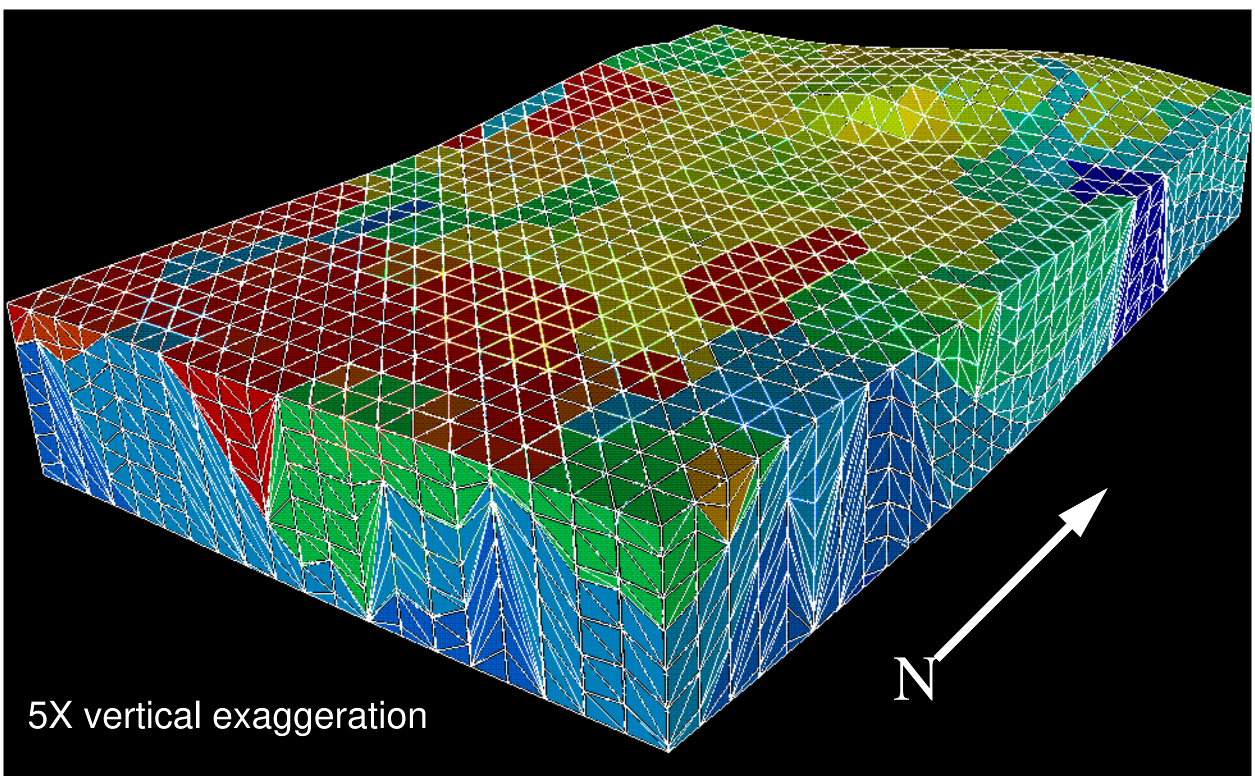

Figure 4-1. Saturated-zone computational grid with 9,279 nodes and 51,461 tetrahedral elements. The upper and lower buffer zones have been removed for visualization.

The permeability of the various units is listed in Table 4-2.

Table 4-2. Permeability and Volume of the Geologic Materials

Material number	Name	Permeability (m^2)
2	Granites	3.5e-14
3	Lower carbonate aquifer	3.3e-12
4	Quartzite confining unit	2.0e-15
5	Lower carbonate aquifer	3.3e-12
6	Eleana confining unit	5.5e-19
7	Lower carbonate aquifer	3.3e-12
8	Upper carbonate aquifer	6.7e-13
9	Leaky confining unit	2.9e-14
10	Lower volcanic confining unit	1.0e-16
11	Lower volcanic aquifer	5.0e-13
12	Middle volcanic confining unit	1.9e-16
13	Middle volcanic aquifer	5.9e-15
14	Upper volcanic confining unit	1.0e-18
15	Upper volcanic aquifer	5.9e-15
16	Basalts	4.5e-14
17	T limestone confining unit	1.0e-14
18	Playa deposits	3.0e-16
19	Alluvium	6.6e-14

Although a calibrated model must have appropriate heads at each inlet and outflow boundary, to test the resolution of the various grids used, the actual pressure differential between the north and south is not important. For simplicity, a pressure difference of 15 MPa is used for all simulations in this grid resolution study. The isothermal model is run to steady state and the flow out of the model is compared for each grid. The effect of gravity on the fluid flow is ignored for this numerical experiment. The problem was designed to study the errors made only in the representation on the hydrostratigraphy. This was achieved by specifying pressures on the north and south faces of the grid. Thus, the solution is a linear variation in pressure with a corresponding constant flux. Tests with homogeneous meshes confirmed this result. The differences in reported fluxes are a result only of representation errors of the hydrogeologic units. The outlet flux was chosen as the parameter to compare because this parameter is likely to be a primary factor in assessing radionuclide transport to the accessible environment.

4.6 Structured Grid Results

Six structured grids were constructed using GEOMESH, and hydrostratigraphic material properties are interpolated onto them. The number of nodes in the *x*, *y*, and *z* directions are chosen so that the nodes in the *z*-direction are equal to the number in the *x*-direction. The nodes are connected into tetrahedral elements. The grid details are shown in Table 4-3. For visual comparison, the stratigraphic model was given in Figure 3-3, the material distribution for grid 5 is shown in Figure 4-2.

Table 4-3. Grid Resolution Details

Grid number	Total number of nodes	Number of nodes, *x* & *z*	Number of nodes, *y*	Spacing of nodes, *x* & *y* (m)	Spacing of nodes, *z* (m)
1	96	4	6	3333	696
2	175	5	7	7500	521
3	1053	9	13	3750	260
4	7225	17	25	1875	130
5	23125	25	37	1250	87
6	40500	30	45	1000	70

The interpolation algorithms work by determining the material number of the element of the original grid that the structured-grid node is located within. Any nodes from the structured grid that fall outside the original grid geometry are assigned a material number of 20. Because the nodal locations are different for each of the six grids constructed, the volumes of the resulting materials change from grid to grid. The finer the structured mesh gets, the more closely the volumes of the materials match those of the stratigraphic model (Figure 4-3). It is also evident from Figure 4-3 that materials with large volumes are less affected by low-resolution grids than small volume units.

Each of the six grids is used to model flow through the saturated zone. A pressure difference of 15 MPa was applied on the north and south boundaries. The resulting fluid flow out

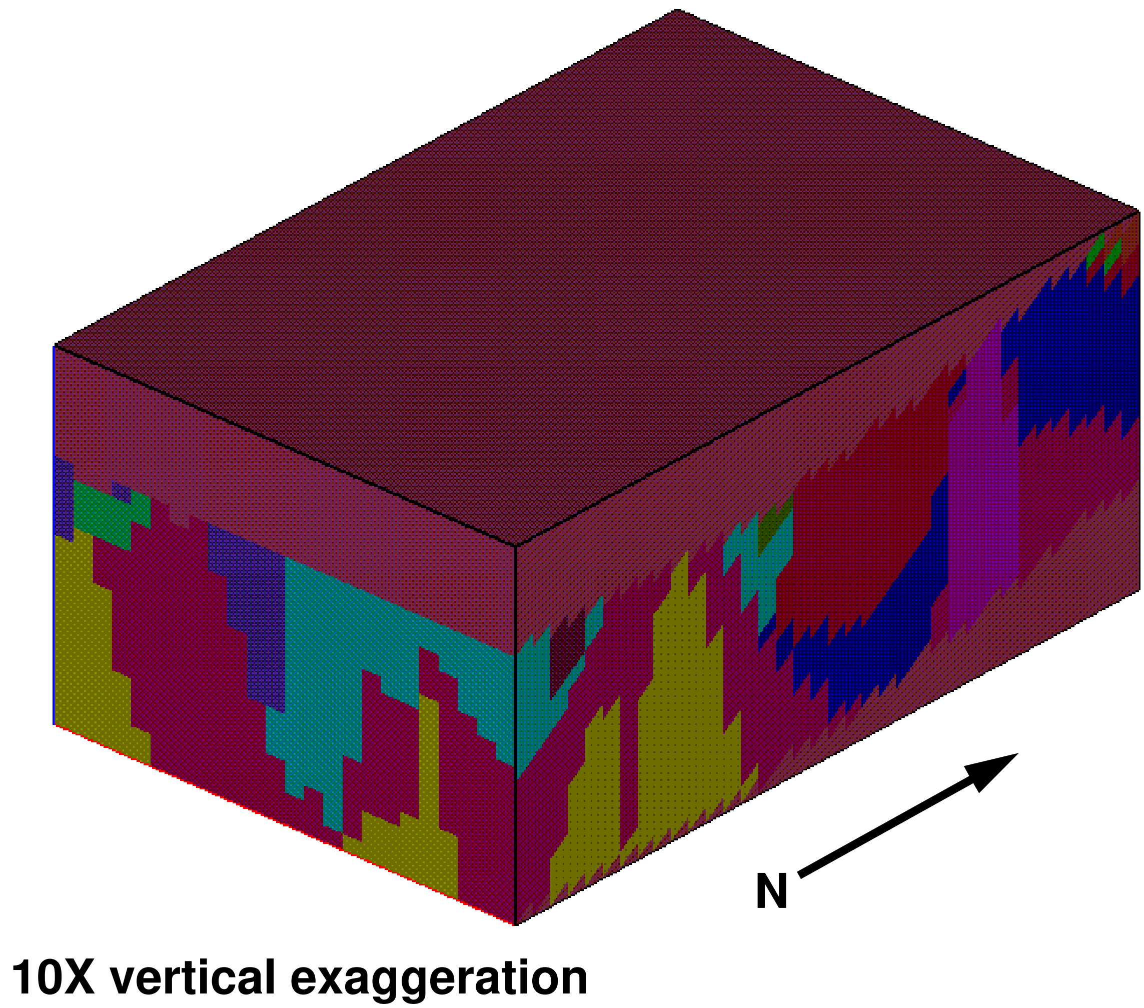

Figure 4-2. Grid 5 of Table 4-3 with material properties interpolated from the geologic framework model.

of the model is used to compare the effectiveness of each grid in representing the effects of the hydrostratigraphy on flow behavior. This flow was obtained by summing the outflow at the south boundary of the model. The resulting flow from each grid is shown in Figure 4-4. The curve shows asymptotic behavior at higher resolution. Because higher grid resolution is more expensive,

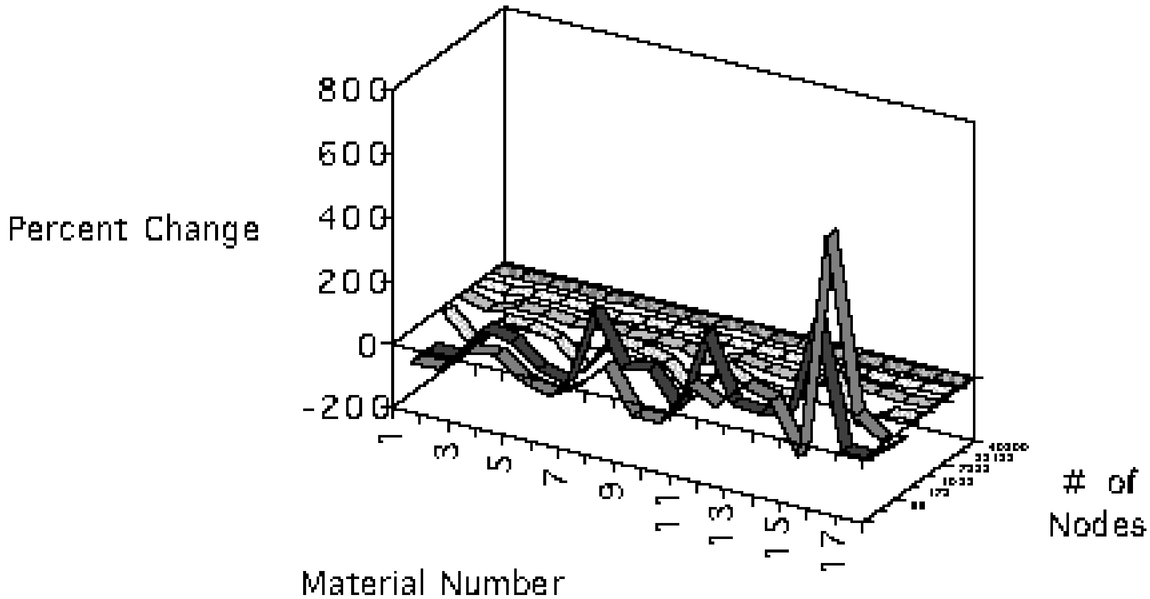

Figure 4-3. The percent change of each material's volume compared to the original material volume is affected by the grid resolution.

Figure 4-4. Flow out of models represented by structured grids. Increasing resolution results in convergence of mass flux towards an asymtotic value.

we can use this type of analysis to determine what the desired accuracy is and at what resolution that accuracy would be attained.

The results of the flux changes with grid resolution can be more easily understood in terms of average grid spacing. The range of grid spacings in the vertical direction range from 696 m to 70 m. The results of this study suggest that for saturated-zone computations, 100-m vertical grid resolution may be sufficient if structured or finite-difference gridding is used. This resolution is a finer grid than is commonly used in saturated-zone simulations of Yucca Mountain. In Section 4.7 we present runs with unstructured-grid representations to determine the resolution necessary for unstructured grids. It is anticipated that the restrictions of grid resolution will be somewhat relaxed if the stratigraphy is captured directly in the unstructured numerical grid. However, note also that this grid resolution study was conducted using total outflow water flux. If a criterion based on radionuclide transport was used, the result would most likely imply the need for higher grid resolution due to the nature of simulating transport using the advection-dispersion equation. Selective grid refinement in the region near the repository and close to the water table in the pathways to the accessible environment will be required for radionuclide transport. Future studies will shed additional light on this requirement.

4.7 Unstructured Grid Studies

As stated in Section 4.6, it is anticipated that the unstructured grid would produce closer flux agreement between grids of different resolution than the structured study mentioned above. To investigate this hypothesis, a finer-resolution model was generated by refining the geological model SFM. This model has approximately 2X resolution in the x, y, and z directions. The finer model is shown in Figure 4-5. The volume of each stratigraphic unit is identical to the lower-resolution model. The boundary conditions used are the same as described in Section 4.6—that is, a 15 MPa difference between the north and south faces with no flow on the top, bottom, east, and west. Again, we compare the flux flowing out of the south face. The results were 3290 kg/s for

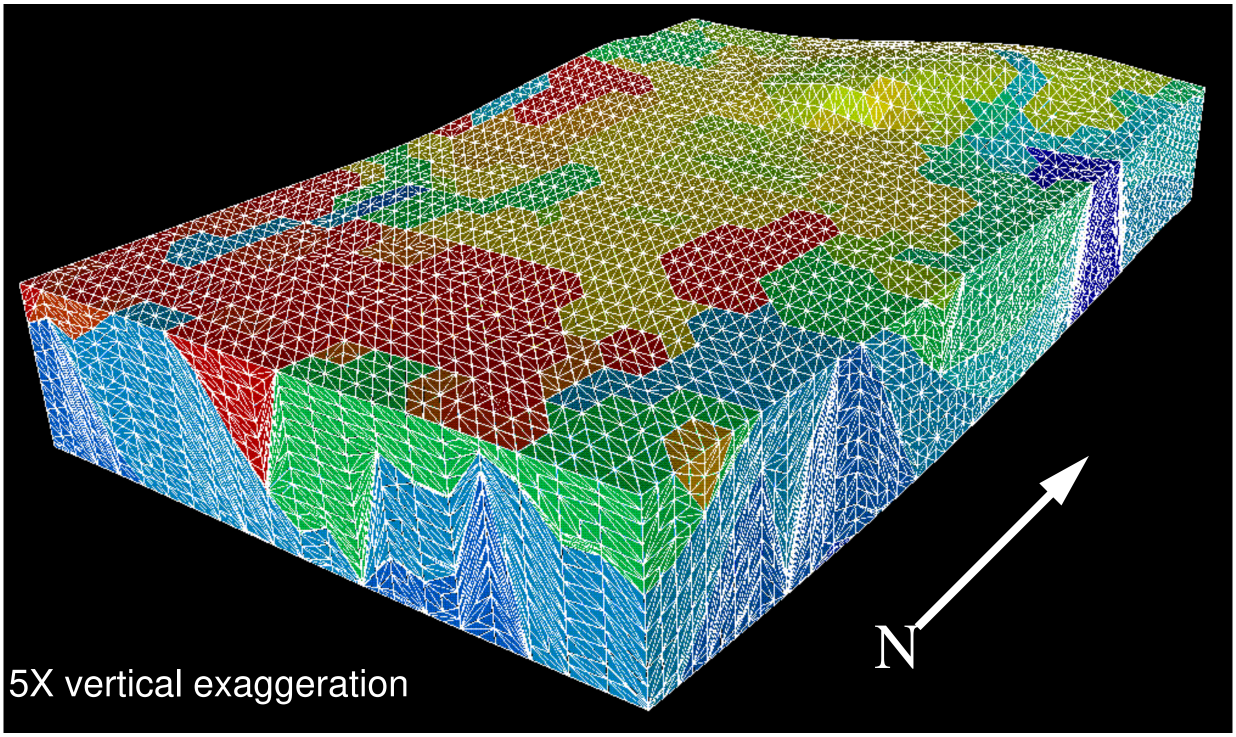

Figure 4-5. High-resolution grid with 49,895 nodes and 293,409 tetrahedral elements.

the lower-resolution model (9279 nodes) and 3760 kg/s for the higher-resolution model (49,895 nodes). The flow rates differ by about twelve percent. The results indicate that the flow calibration with the lower-resolution model is sufficient but some caution is warranted. Time constraints precluded additional resolution studies. As indicated in Section 4.6, transport simulations would require additional resolution. These studies do point to a need to systematically study grid refinement and its relation to both flow and transport.

4.8 Grid Refinement Around Plumes

To adequately model contaminant transport through porous media, a computational grid will require refinement beyond that required for flow modeling. This requirement is true of the grid used for USGS/LANL site-scale saturated-zone flow simulations of the regional aquifer beneath Yucca Mountain (Czarnecki et al., 1997). We have developed an approach for grid refinement that refines only that part of the grid where most contaminant migration occurs, thus minimizing the number of nodes added to the grid to assure an accurate transport solution. The refinement technique uses the results of a transport solution computed on a grid that is expected to be too coarse for an accurate transport solution. The preliminary coarse grid is then refined in the region where most contaminant migration occurs (e.g., within a specified isoconcentration surface). The flow and transport solution is recalculated on the refined grid. This grid may then be refined again within an isoconcentration surface that is generally of lower concentration than used for the initial refinement. Refinement is complete when the breakthrough curves computed at some compliance point no longer vary within a specified tolerance level. This approach is a form of adaptive mesh refinement that uses the problem solution to guide the refinement process. The technique, which uses the GEOMESH/X3D grid-generation system, was first tested on a rectangular grid with a single porous medium. This case is discussed, as it is useful in explaining the refinement methodology. The technique, tested below, will be employed in FY98 to the 250-m sampled SFM currently being developed by the USGS.

4.8.1 Single-material grid

In this section, we discuss the grid-refinement technique using the single-material grid as an example. We start with a uniform, single-material grid of 5793 nodes and 36,864 tetrahedral elements. This grid has the same external dimensions as the desired site-scale grid. A pressure gradient, of the same magnitude as the site-scale saturated-zone model, is applied across the north and south boundaries to create a steady flow field. Then, contaminant of uniform concentration is introduced into a few upstream nodes that are meant to represent the entry region of radionuclide migrating from the potential repository through the vadose zone and into the aquifer. The transport calculation is run to steady state, resulting in a plume that identifies all nodes where contaminant travels through the grid. Figure 4-6 shows the resulting plume for this coarse uniform grid.

The coarse grid was then refined within an isoconcentration surface of $C = 0.1$. The steady flow and transport solutions were recomputed on the resulting grid. A second level of refinement was completed within the $C = 0.05$ isoconcentration surface, and again, the flow and transport solutions were updated. Figure 4-7 shows the resulting 28,511-node grid after two levels of

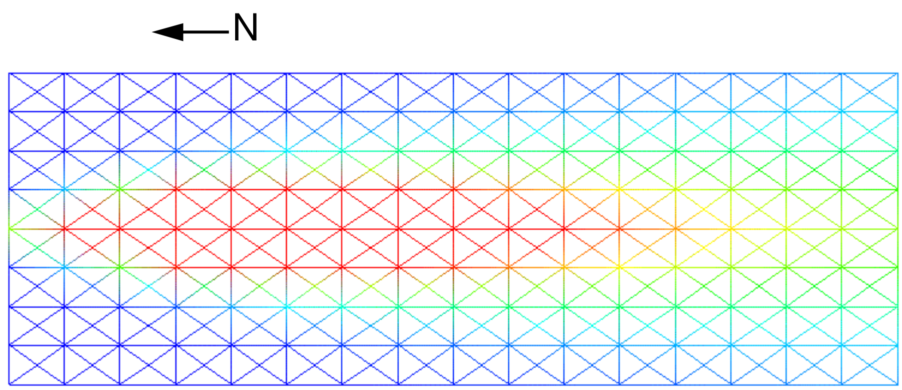

Figure 4-6. Plan view of steady-state transport solution on the coarse, single-material grid.

refinement, first at $C = 0.1$ and then at $C = 0.05$. The top view shows that the plume primarily travels in the direction of flow with little transverse spreading for this single-material case. Approximately 25% of the volume has undergone two levels of refinement, and an additional 25% of the grid that surrounds the center has undergone one level of refinement. The outer 50% of the grid is unchanged because the plume does not migrate to that region of the domain. The side view shows that most of the vertical refinement occurs near the surface even at the downstream boundary. Because this process is experimental, several other refined grids were generated using this same technique with differing isoconcentration surfaces. This approach allowed optimization of the concentration criteria.

A criterion is needed to determine when the grid is adequately refined. We have chosen to look for convergence in the breakthrough curve at a downstream compliance point. Figure 4-7 shows the breakthrough monitoring location, which is the uppermost, central node of the grid at the downstream boundary. We found that the original constant-concentration source used for grid refinement results in different solute mass-flux input rates with the different grids. Therefore, transport solutions were rerun with the various grids using constant tracer flux so that each

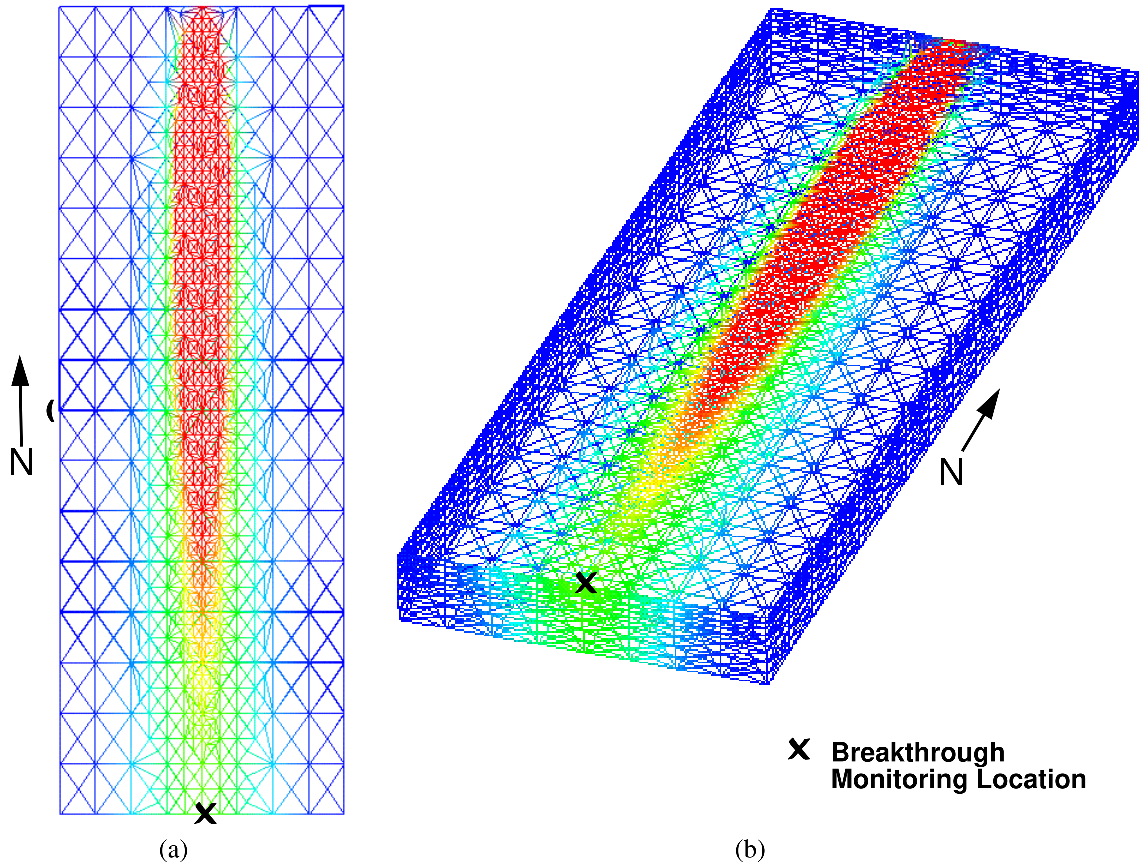

Figure 4-7. Single-material grid after two levels of refinement within isoconcentration surfaces of 0.1 and 0.05 with both (a) plan view and (b) perspective view.

simulation would receive the same mass, and the breakthrough curves could then be compared. Figure 4-8 shows breakthrough curves for several of the grids with the legend indicating the number of times the grid was refined (once or twice) and the isoconcentration surfaces used. As the grid is refined, breakthrough to the monitoring point advances slightly in time and the steady-state breakthrough concentration generally increases. This result occurs because the plume exhibits less numerical dispersion around its centerline and with depth. There is little difference between the solutions for the grids with 28,511 (0.1, 0.5) and 57,450 (0.05, 0.01) nodes indicating that the 28,511-node grid is adequately refined.

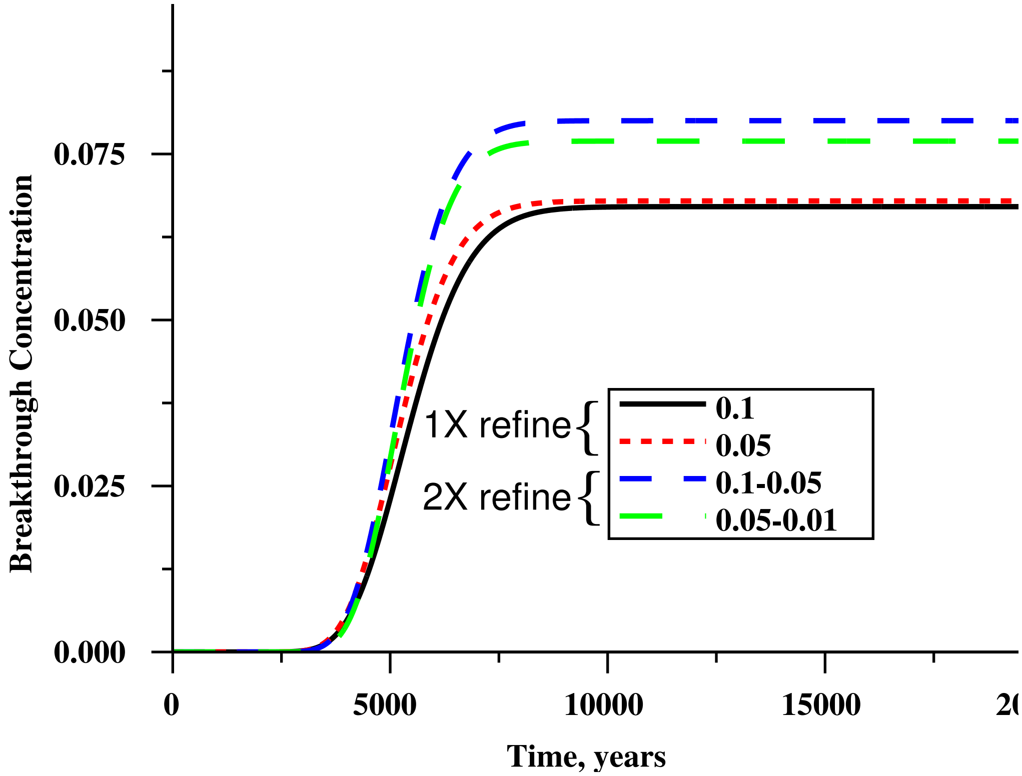

Figure 4-8. Breakthrough curves for various refinement levels of the single-material grid. Isoconcentration levels used to define refinement zone are given in the legend.

4.8.2 Multiple-material grid.

Future work will apply the refinement technique discussed above to the USGS/Los Alamos multiple-material saturated-zone model. Refinement will be based on the concentration of a steady plume generated with the calibrated flow field. Nodes added during refinement are assigned material properties based on the original Stratigraphic Framework Model discussed previously. The original nodes remain in the grid and retain their material properties. Refinement of the USGS/Los Alamos model was not pursued for this year's study. The coarse 1500-m spacing of the current stratigraphic framework model (SFM) is inadequately refined to justify refinement for transport simulations. An updated SFM with 250-m spacing will be incorporated in future work (see Sections 3.5 and 6.5). This refined SFM has adequate stratigraphic information to work ideally with the concentration adaptive mesh refinement technique.

4.9 Conclusions

Grid resolution was found to be a critical issue for both flow and transport. The ability to resolve heterogeneous geologic units was a function of grid resolution. Grid-resolution studies were carried out with both unstructured and structured grids. It was found that the USGS-calibrated flow model produced fluxes that changed little by resolving the grid and was thus deemed of sufficient resolution for flow simulation. A new method was described to locally resolve grids for transport simulations. The main application of this technique will be for refining the revised site-scale model for transport calculations.